Liquid Crystals
Publication details, including instructions for authors and subscription information:
http://www.informaworld.com/smpp/title~content=t713926090

A fractal model for the molecular organization in the alkylbenzenesulphonate/electrolyte/water system

D. Tezak; S. Puncec; M. Martinis

Online publication date: 06 August 2010

To cite this Article Tezak, D. , Puncec, S. and Martinis, M.(1997) 'A fractal model for the molecular organization in the alkylbenzenesulphonate/electrolyte/water system', Liquid Crystals, 23: 1, 17 — 25
To link to this Article: DOI: 10.1080/026782997208622
URL: http://dx.doi.org/10.1080/026782997208622

LIQUID CRYSTALS, 1997, VOL. 23, NO. 1, 17–25

A fractal model for the molecular organization in the alkylbenzenesulphonate/electrolyte/water system

by Đ. TEŽAK*, S. PUNČEC† and M. MARTINIS‡

†Department of Chemistry, Faculty of Science, University of Zagreb, Marulićev trg 19, P.O. Box 163, 10001 Zagreb, Croatia

‡Rugjer Bošković Institute, Bijénicka C.54, P.O. Box 1016, 10001 Zagreb, Croatia

(*Received 14 August 1996; in final form 4 February 1997; accepted 17 February 1997*)

Under conditions where individual molecules are no longer soluble, the association of amphiphiles occurs as a sequence of growth and aggregation processes: the formation of dimers, bilayers and multilayer assemblies culminates with the production of myelin cylinders and chains or spherulitic arrays of focal-conic units. We have examined this process using the alkylbenzenesulphonate/electrolyte/water system as a model. The phase diagram was obtained using optical microscopy. The kinetics of the aggregation process were followed by light-scattering measurements and the structures of the one- and two-phase regions were examined by optical microscopy and freeze-fracture electron microscopy. The fractal nature of the aggregation process was investigated using an indirect Fourier transform study of the light-scattering data. The fractal character of the whole self-assembly process was confirmed and an experimental value of 2·17 was determined for the fractal dimension (in close agreement with the expected theoretical value of 2·16).

1. Introduction

We have recently proposed a multifractal model for the aggregation of alkylbenzenesulpnonate (ABS) molecules in lamellar mesophases [1]. It is well known that bilayers can form a variety of structures and undergo many structural transitions [2], different lyotropic mesophases corresponding to packing defects and unlimited large deformations [3] such as the focal-conic arrays and the edge dislocation [4], or to the possibility that a bilayer can fold into several global structures like cubic phases [5, 6], vesicles [7–9], sponge phases [10, 11], bicontinuous structures with simple cubic symmetry [12] and myelin figures [2]. Although Fournier [13] described recently the way in which focal-conic units of lamellar phases assemble to give larger structures, these structures were already understood by Sir W. Bragg [14]. In this paper the arrangement of a set of focal-cones has been shown geometrically within a pyramid, and it follows closely either the actual arrangement within a polygon as obtained by using crossed polarizers or is represented by focal-conic texture. Although focal-conic arrangements have been studied in smectic phases [13, 14], the same structures can be applied to lamellar phases, while such textures have also been found in the viscous samples of lamellar phases separated from supernatant solutions.

*Author for correspondence.

ABS forms mostly lamellar phases in binary systems with water [15]. In ternary systems, with the addition of an electrolyte to the binary ABS/water system, the formation of lamellar phases (L_α) also occurs [16, 17]. In addition, an electrolyte can form a salt with a surfactant under defined conditions. A general precipitation diagram showing the interaction of dodecylbenzenesulphonic acid and metal nitrates is given in figure 1 and shows the concentration-dependence of the various phases. Usually, high concentration of an electrolyte (above 10^{-1} mol dm^{-3}) causes the formation of solid crystals (KS), with a very fast nucleation of crystalline nuclei. The liquid crystalline phase appears above the critical micellar concentration (c.m.c.) in the equimolar concentration region. Although the solid crystalline salts require the stoichiometric condition, this is not strictly necessary for liquid crystalline phases (the results obtained with cadmium dodecylbenzenesulphonate will be published). The structure of both the crystalline and the liquid crystalline phases (L_α) of magnesium dodecylbenzenesulphonate shows a basic bilayer organization with interplanar spacings of $(30{\cdot}6 \pm 0{\cdot}3)$ and $(33{\cdot}2 \pm 0{\cdot}6)$ Å, respectively. At high surfactant concentration, an optically isotropic, inverse cubic phase (IC) with a spacing of $(34 \pm 0{\cdot}6)$ Å has been observed [18].

The influence of temperature on the nucleation processes [19], in the case in which the solutions have been mixed together at higher temperatures showed that

0267–8292/97 $12·00

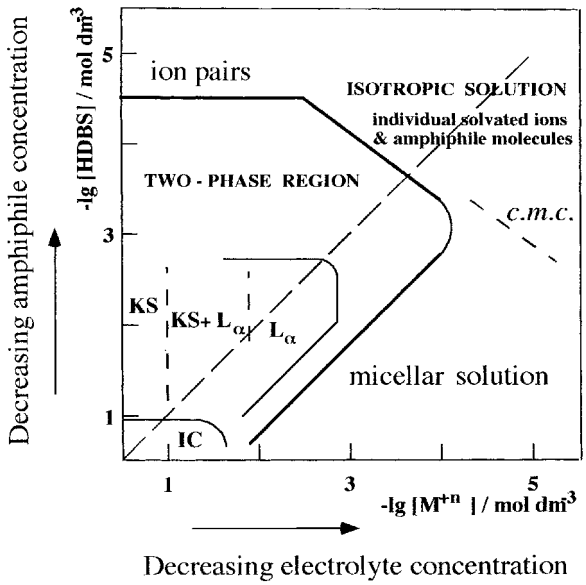

Figure 1. Schematic representation of the phase diagram contours of the HDBS/electrolyte/water system. In the most dilute region at the top right, there are individual hydrated ions and individual amphiphile molecules; at the top left, at high electrolyte concentrations, the ions are associated into ion pairs and higher aggregates; at the bottom right there is a micellar solution. At higher amphiphile concentrations there are the lamellar L_α phases, the crystalline solid, KS, and at the highest amphiphile and electrolyte concentrations, an inverse cubic phase IC.

the formation of crystal nuclei is favoured by higher temperatures, due to the increased energy.

In the present paper we propose a model for the formation of lamellar phases by alkylbenzenesulphonates. The dynamics of the amphiphile association show that this can not be treated as a continuous process [20]. A fractal model for the self-association process is proposed on the basis of the indirect Fourier transform (IFT) of the light-scattering data, polarization microscopy, freeze-fracture transmission electron microscopy (FFTEM) and X-ray diffraction measurements.

The mathematical model being tested in this paper was analysed in the Guinier regime in terms of the scattering intensity from a single spherulite cluster, as well as in the intermediate regime in terms of total scattering intensity from a polydisperse fractal sample. In order to study structural details of a polydisperse sample we consider the pair distance distribution function.

2. Experimental

2.1. *Materials*

Lyotropic liquid crystalline phases are usually formed in binary systems by mixing ABS with water [15], or in ternary or multi-component systems by mixing the aqueous solutions of ABS above the c.m.c. with metal nitrates in an equimolar ratio [17].

The aqueous solution of dodecylbenzenesulphonic acid (HDBS), a commercial product of Ventron, Germany, was used as the surfactant. The standardization was performed potentiometrically with standard NaOH solution. Analytically pure $Mg(NO_3)_2$ from E. Merck, Darmstadt, dissolved in water, was standardized complexometrically. More detailed information about chemicals and the procedures has been published earlier [16]. Doubly distilled water was used in all experiments.

2.2. *Methods*

The onset of dimerization, the critical micellar concentration, as well as the patterns of size, mass and volume distribution of particles, were determined by light-scattering, using the static (SLS) and dynamic (DLS) light-scattering photometer Otsuka 700. The conditions of measurement have been described earlier [1]. For calculations using the light scattering data, the particle size distribution was taken as mono-modal. Although some of the systems showed bi-, and tri-modal distribution, it was found that the number of small particles in any distribution was sufficiently predominant to justify this. A fractal study of the light-scattering data was carried out using IFT.

The thicknesses of the lamellar bilayers were determined using a standard Siemens X-ray diffractometer and Si-crystal monochromatized CuK_α radiation. Freeze-fracture transmission electron microscopy (FFTEM) photomicrographs were obtained by courtesy of the University of Braunschweig, Germany. The liquid crystalline textures of the macro-phases were determined using a Leitz Wetzlar optical microscope with polarizing equipment.

3. Results and discussion

3·1. *Aggregation model*

HDBS begins to form dimers at concentrations above 4×10^{-4} mol dm^{-3}, and the c.m.c. is $1{\cdot}7 \times 10^{3}$ mol dm^{-3} [15]. The liquid crystalline phase separates out above the c.m.c. in the samples containing electrolyte. In figure 1, the equilibrium precipitation limit and the regions of different precipitated phases from the supernatant solution are shown schematically for bi-, and trivalent cations. The X-ray diffraction contains several orders of sharp maxima which confirm that the liquid crystalline phase is lamellar [21]. Generally, the interplanar distance for lamellar phases of all HDBS-metal salts investigated (uni-, bi-, and tri-valent) was 32·1–34·6 Å [17]. For comparison, the calculated length of the linear C_{12} molecule is 26·5 Å. Considering the

hydrocarbon chains are flexible, it can be assumed that a water layer between the hydrocarbon parts within the bilayers amounts to 3–4 Å. It can also be assumed that the hydration forces of the cations can cause small differences in thickness of the aqueous part within the bilayer.

The dynamics of the development of a lamellar phase can be considered in terms of a hierarchy of effects: the molecular association in solution, the growth of primary particles, and the aggregation of primary particles into secondary structures. This was shown by following the kinetics of liquid crystal formation which develops at consecutive time intervals, including fast growth and steady-states [20]. This process is represented in the scheme:

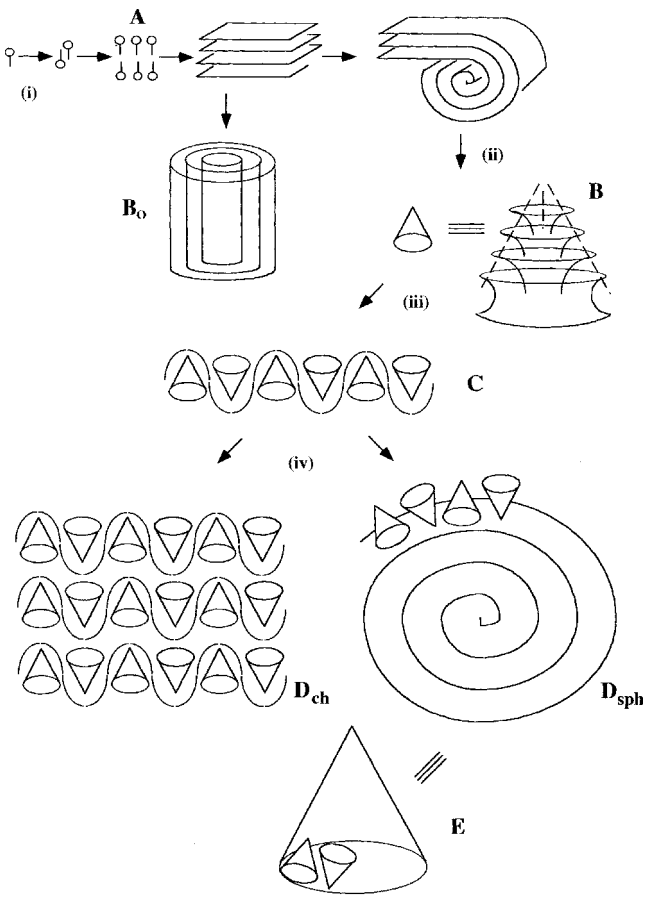

Scheme. Schematic representation of the association steps of ABS surfactants in solution: (i) dimerization, formation of uni-lamellar, multi-lamellar phases (**A**), and myelin cylinders ($\mathbf{B_o}$); (ii) folding of multi-lamellae to a globular (focal-conic) form (**B**); (iii) aggregation of globular primary particles into the primary aggregates, i.e. necklace chains (**C**); (iv) aggregation into secondary aggregates ($\mathbf{D_{sc}}$ and $\mathbf{D_{sph}}$ represented as **E**).

(1) According to the FFTEM micrographs in figures 2(*a*)–2(*c*) a 30 Å bilayer can be considered as the basic structural unit of both a flat (**A**) or a bent lamellar phase (**B**). The bilayers form a multilayer. The depth of a 'basic multilayer stack' (one of them is denoted by arrows in figure 2(*a*)) amounting to either 90 or 120 Å was calculated from flat and from bent lamellar 'layers', corresponding to three or four bilayers in the basic stack.

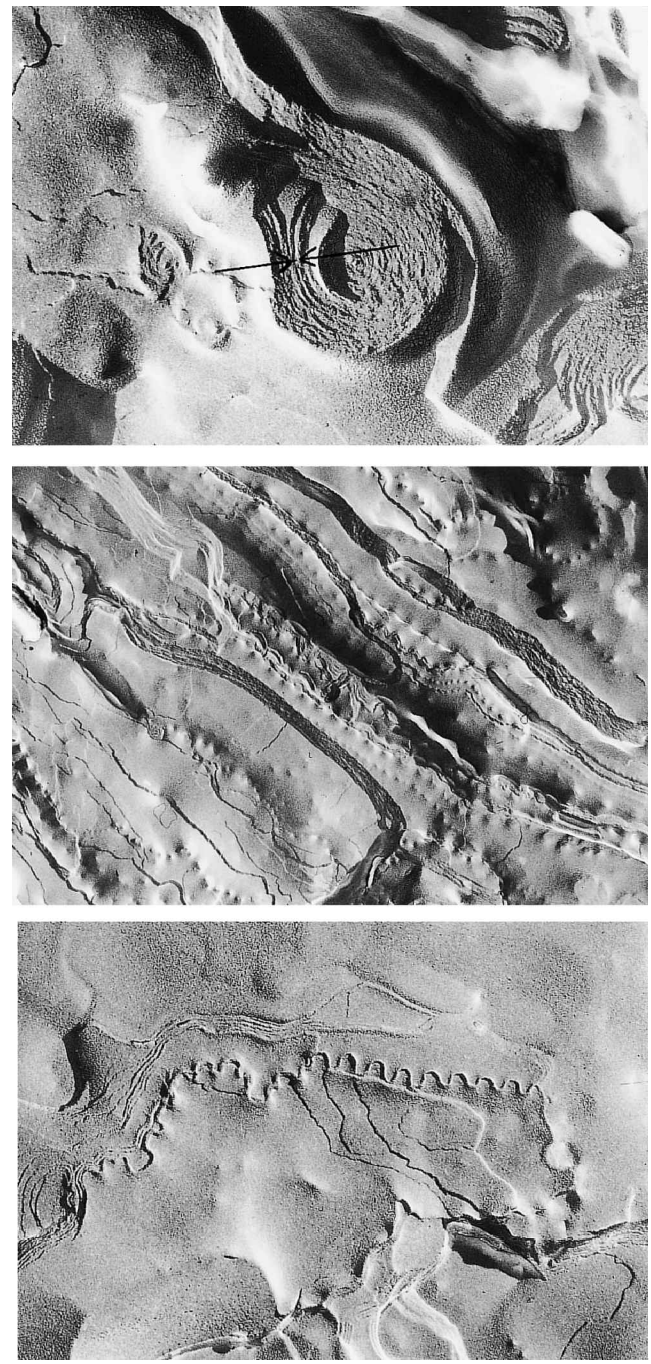

Figure 2. Freeze fracture transmission electron micrographs of the sample containing $[Mg(NO_3)_2] = 6 \times 10^{-2}$ mol dm^{-3} and $[HDBS] = 6 \times 10^{-2}$ mol dm^{-3}; total mag: (*a*) 110 000×, (*b*) 42 000×, (*c*) 86 000×.

(2) The formation of a *primary spherulite* (**B**) involves the bending of the lamellar multilayer (figure 2(*a*)). According to Fournier and Durand [13] it is very probable that such a structure is a cone. It is shown in figure 2(*a*) that some multi-lamellar structures do not fold into focal-conic units; they are represented by the parallel lines. In addition, it is apparent from the rows of small spherical images in figure 2(*b*) that only monodisperse particles are allowed to form a chain aggregate.

(3) The aggregation of *primary spherulites* into a secondary structure that can produce a chain-like aggregate resembling a *necklace* (**C**) is shown in the TEM micrograph in figure 2(*c*). The sinusoidal trace represents the place where the focal-conic units originally were before the freeze-etching. It can be determined from the micrograph that the depth of this particular chain is 440 Å, which is a reasonable size for the basic multilayer to be folded into a cone. In addition, the typical lamellar myelin forms are also present in some samples. It can be assumed that myelin cylinders can include one folded bilayer, or even a multilayer, schematically represented by hollow cylinder ($\mathbf{B}_o$) in the scheme; the myelin forms can be seen in the optical photomicrographs (figures 3(*a*), 3(*b*) and 3(*c*). Such structures are also assumed [3, 6] to be present as basic forms.

(4) Further aggregation steps include folding of the primary particles, usually chain-like aggregates into either large *secondary spherulites* ($\mathbf{D}_{sph}$) or into parallel *stack aggregates* ($\mathbf{D}_{ch}$). These forms can be seen in figures 3(*d*)–3(*f*). The sizes of these spherulites vary from 2·5 to 60 μm. The appearance of sinusoidal traces in the optical birefringence texture in figures 3(*d*), 3(*e*) and 3(*f*), which has already been observed in many samples [16, 22], reminds us of the similar traces from the FFTEM-micrograph showing presumably the chain-like aggregation of *primary spherulites*. These textures can be considered to represent the chain-like aggregation of *secondary spherulites* or *macrospherulite*. It can be assumed that the curved lines indicate the places where the macro-spherulites are connected together. It can also be assumed that *primary spherulites* can form fractal objects, *secondary spherulites*, as indicated by a cone (**E**) in the scheme. It can easily be imagined that the spiral from ($\mathbf{D}_{sph}$) expanded in three-dimensions can be represented by a cone (**E**) (some primary cones are presented inside the cone (**E**).

3.2. *Fractal approach by the Indirect Fourier Transformation method*

The aggregation kinetics [20], as well as the microscopic observations (the well expressed stepwise aggregation, both by electron and polarizing microscopy), indicate the possibility that these processes generate fractal structure. In this paper we shall appraise means for an indirect Fourier transformation (IFT) [23–25], the assumption of a fractal (multi-fractal) growth and aggregation of the lamellar phase considered recently by us [1].

The data used for the fractal analysis were those obtained from static light-scattering (SLS) described in the previous paper [1] and for particle size determination those from the dynamic light-scattering (DLS) (this work). The basic assumptions concerning our calculation are as follows. (1) The sizes of the *primary spherulites* (figure 2, and the scheme), which are supposed to be focal-conic units, are assumed to be smaller than the wavelength of the incident light which is $\lambda_0 = 488$ nm. The sizes of the cones, calculated from spherical traces from FFTEM micrographs amount to 40–440 nm (figure 2); in addition, it is obvious from the FFTEM photomicrographs that the sizes of most primary particles are even smaller. (2) The cones have been approximated to by spheres having a diameter equal to the radius of gyration.

The average particle sizes exhibiting a Gaussian dispersity distribution from DLS data show an exponential time function; we can consider that after 1 day the system is equilibrated (figure 4).

In the dilute regime, the multiple light-scattering of the spherulite clusters can be neglected, and the total scattering intensity is given by

$$I_t(Q) = \int N_t(M) I(Q, M) \, \mathrm{d}M \qquad (1)$$

Figure 3. Optical photomicrographs showing lamellar phases in equilibrium with the supernatant solution: (*a*) a long, myelin type cylinder bent in several places, $[Mg(NO_3)_2] = 4 \times 10^{-3}$ mol dm^{-3}, [HDBS] $= 6 \times 10^{-3}$ mol dm^{-3}, $t = 20$°C, crossed polarizers + λ-plate at 45°, total mag. 450×; (*b*) the same sample as in (*a*) without polarizers; (*c*) myelin figure presumably formed by twisting the cylinder, this is a different sample but under the same conditions as in (*a*) (except $t = 40$°C); (*d*) chains of secondary aggregates with sinusoidal traces, note the indistinct lines in the centre resulting from a row of particles that are moving very fast and forming a chain-like stick aggregate, $[Mg(NO_3)_2] = 1 \times 10^{-2}$ mol dm^{-3}, [HDBS] $= 2{\cdot}5 \times 10^{-3}$ mol dm^{-3}, $t = 40$°C, polarized light, λ-plate, total mag. 180×; (*e*) texture with chain-like aggregates exhibiting the sinusoidal traces and indicating the connection areas of the single particles, $[Mg(NO_3)_2] = 6 \times 10^{-2}$ mol dm^{-3}, [HDBS] $= 6 \times 10^{-2}$ mol dm^{-3}, $t =$ 5°C, crossed polarizers + λ-plate, total mag. 180×; (*f*) formation of a large globular secondary aggregate by coiling the chains of particles, the difference should be noticed between the coil in the middle of figure 3(*f*) and the spherulitic structure showing maltese crosses, $[Ba(NO_3)_2] = 5 \times 10^{-2}$ mol dm^{-3}, [HDBS] $= 5 \times 10^{-2}$ mol dm^{-3}, $t = 20$°C, crossed polarizers + λ-plate, total mag. 450×.

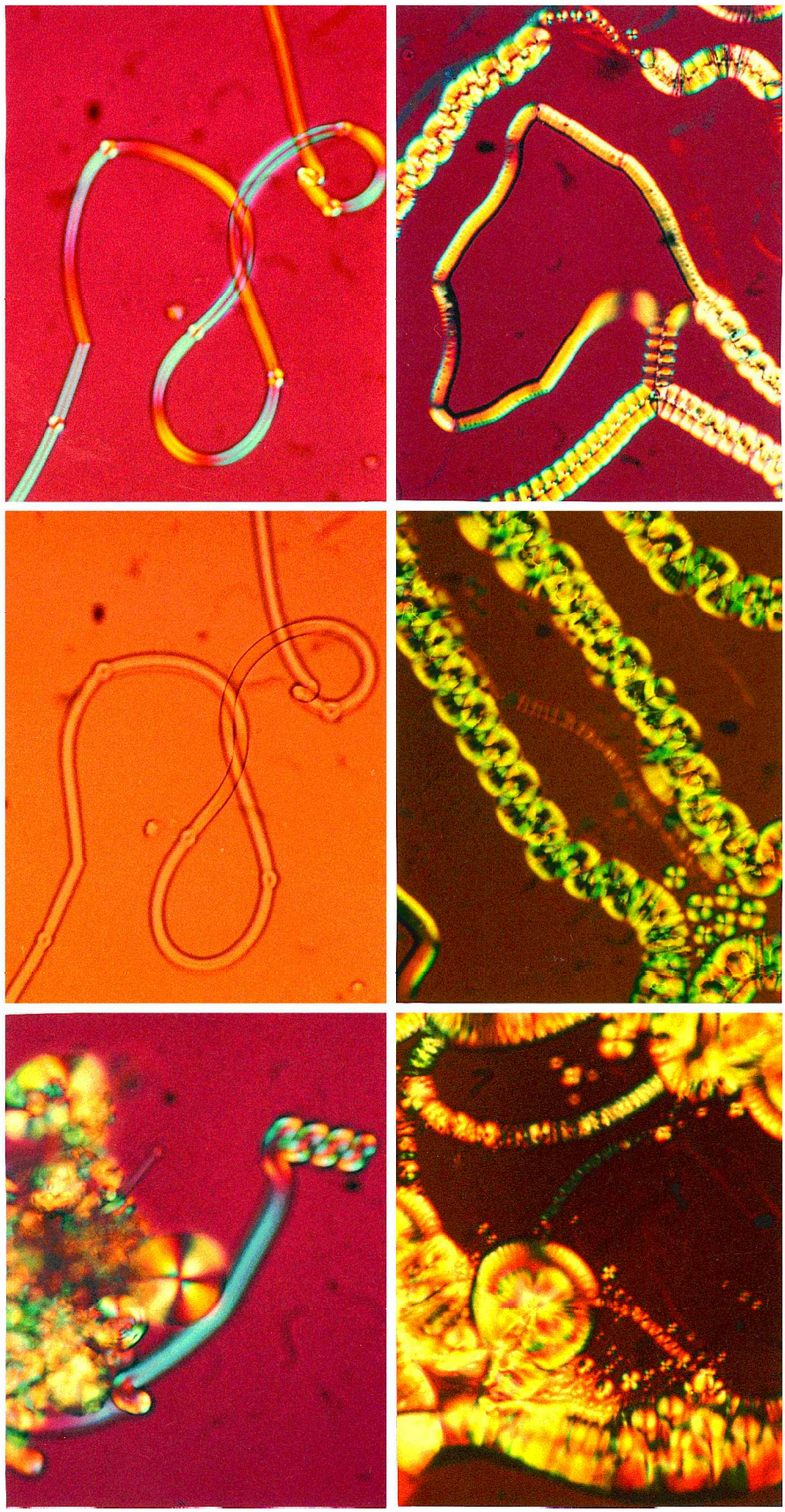

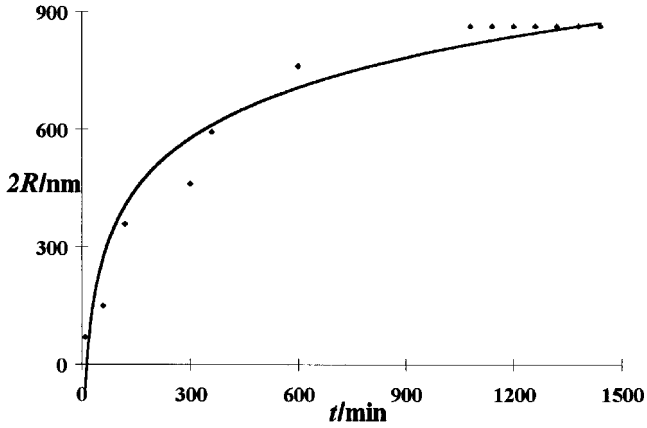

Figure 4. Kinetics of the aggregation, presented as a *particle diameter versus time* plot, for the sample of magnesium dodecylbenzenesulphonate prepared by mixing aqueous solutions of $Mg(NO_3)_2$ ($c = 6 \times 10^{-2}$ mol dm^{-3}) and HDBS ($c = 6 \times 10^{-4}$ mol dm^{-3}). This shows that equilibrium was established after approximately 16 hours, since the maximum particle size does not increase after this time.

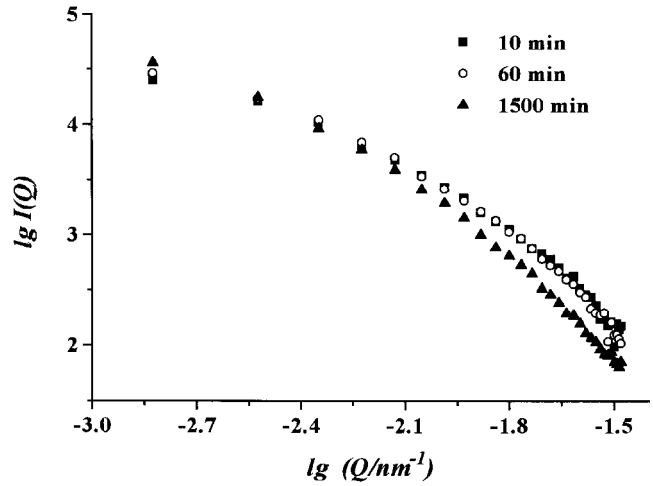

Figure 5. The fractal dimension D of the 'colloidal' liquid crystalline phase, determined from the slope from the *scattering intensity versus length of the scattering vector* plot 1 day after preparation of the sample (the same as in figure 4).

where $Q = (4\pi n/\lambda)\sin(\theta/2)$ *denotes the length of the scattering vector*, n is the refractive index, λ is the wavelength of the incident beam in the scattering medium, and θ is the scattering angle; $N_t(M)$ denotes the number of spherulite clusters of mass M in the scattering volume V at time t. The scattering intensity from a single spherulite cluster of mass M is $I(Q, M) \propto M^2 P[QR(M)]$, where $P[QR(M)]$ denotes the form factor of the cluster of mass M and radius R.

In the Guinier regime corresponding to the condition $QR(M) < 1$ we have

$$I(Q, M) = I(0, M)\left(1 - \frac{1}{3}Q^2R^2(M) + \cdots\right)$$

where $I(0, M) \propto M^2$, and

$$I_t(Q) \propto \rho V M_w(t)\left(1 - \frac{1}{3}Q^2R_g^2(t) + \cdots\right) \quad (3)$$

Here, V is the scattering volume, and ρ the mass per unit volume, i.e.

$$\int MN_t(M)\,\mathrm{d}M = \rho V. \quad (4)$$

The quantities $M_w(t)$ and $R_g^2(t)$ are defined as

$$M_w(t) = \frac{1}{\rho V}\int M^2 N_t(M)\,\mathrm{d}M \quad (5)$$

and

$$R_g^2(t) = \frac{1}{\rho V M_w(t)}\int R^2(M)\,M^2 N_t(M)\,\mathrm{d}M, \quad (6)$$

and represent the average cluster mass or molecular mass and the z-average cluster radius of gyration at time t, respectively.

If $R(M) \propto M^{-d_f}$, where d_f is the fractal dimension of the cluster, and $N_t(M) \propto M^{-\tau}$, where τ is the polydispersity exponent [26, 27], then there is a power law relation between M_w and R_g given by

$$M_w(t) \propto [R_g(t)]^{(3-\tau)d_f}. \quad (7)$$

In the intermediate regime, where $QR_g(t) \geq 1$, the total scattering intensity from a polydisperse fractal sample is

$$I_t(Q) \propto Q^{-D} \quad (8)$$

where the exponent $D = (3 - \tau)d_f$ may be considered as an effective fractal dimension of the ensemble of clusters having on average a mass $M_w(t)$ and a radius $R_g(t)$. In order to extract d_f from the measured exponent D, it is necessary to perform a separate determination of the exponent τ by studying in detail the particle size distribution $N_t(M)$ in the sample.

Experimentally determined fractal dimensions, obtained from SLS data, are given in table 2. The change in the slopes for three determinations at three different times are presented in figure 5, and show that the sample was equilibrated after 1 day; consistently, the fractal dimension can be considered to be $D = 2{\cdot}16$. The fit between values of $\lg Q = 2{\cdot}4$–$1{\cdot}8$, demonstrating the fractal scaling at short length scales, can be considered as relevant to two dimensional, diffusion limited cluster aggregation (DLCA), according to Earnshaw's studies of a structure factor in colloidal aggregation [28]. In addition, the fractal dimensions of the clusters determined by SLS measurements on Ludox colloidal

Table 1. Structural form and size of the possible aggregation steps proposed for the amphiphile (to fit the Scheme)

Sign	Form	Size/nm	Method
Processes: ASSOCIATION and GROWTH			
A	monomer	2·65	calculated
A	dimer		light scattering
A	bilayer	3·3	X-ray diffraction
A	flat lamellae: 3–4 bilayers	9–12	FFTEM
$\mathbf{B_o}$	myelin cylinder		polarization microscopy
B	primary spherulite: cone	[a]70–330	FFTEM
Process: AGGREGATION			
C	cones connected into chain	[a]	FFTEM
$\mathbf{D_{ch}}$	stack of chains	109–136	light-scattering (IFT)
$\mathbf{D_{sph}}$	secondary spherulite: top view	[b]	polarization microscopy
$\mathbf{E = D_{sph}}$	secondary spherulite: side view		

[a] Primary spherulites differ in size, but only the monodisperse spherulites form the chains.
[b] The sizes of secondary spherulites from polarizing microscopy data were found to be 2·5–60 μm in diameter.

Table 2. Fractal dimensions of the liquid crystalline sample of Mg dodecylbenzenesulphonate: [$Mg(NO_3)_2 = 6 \times 10^{-4}$], [HDBS $= 6 \times 10^{-4}$] (concns. in mol dm^{-3}).

t/min	D	R[a]	SD[b]
10	1·77	0·9975	0·025
60	1·84	0·9982	0·022
1440	2·16	0·9954	0·041

[a] R = correlation factor.
[b] SD = standard deviation.

aggregates showed that the linearity in the $I(Q)$ versus Q plot can also be fitted over a narrow range [29].

In order to study structural details (fractality) of such a polydisperse sample, we consider the pair distance distribution function, $p_t(r)$, calculated from the scattering intensity, $I_t(Q)$, via the indirect Fourier transformation (IFT). The relation between the scattering intensity, $I_t(Q)$, and $p_t(r)$ for non-oriented clusters is given either by the Fourier transformation (FT)

$$I_t(Q) = 4\pi \int_0^\infty p_t(r) \frac{\sin(Qr)}{Qr} \mathrm{d}r \qquad (9)$$

or by IFT if $p_t(r)$ is calculated from $I_t(Q)$

$$p_t(r) = \frac{1}{2\pi^2} \int_0^\infty I_t(Q)(Qr)\sin(Qr)\mathrm{d}Q. \qquad (10)$$

It is easy to see that in this case

$$p_t(r) = \int p_M(r) N_t(M) \mathrm{d}M \qquad (11)$$

where $p_M(r)$ is the pair distance distribution function [27] of a cluster of mass M. The fractal structure of the sample is reflected in the behaviour of the pair distance function

$$p_t(r) = r^{D-1} f(r/\xi(\tau)) \qquad (12)$$

where $f(r/\xi(\tau))$ is a scaling function that is assumed to decay rapidly for $r > \xi(t)$, and is a simple constant for $r \ll \xi(t)$. Here $\xi(t)$ is a cut-off length scale at a time t which is related to the average radius of gyration $R_g(t)$ by

$$R_g(t) = A_D \xi(t) \qquad (13)$$

where a constant A_D is

$$A_D^2 = \int x^{D+1} f(x)\mathrm{d}x \Big/ \left(2 \int x^{D-1} f(x)\mathrm{d}x\right) \qquad (14)$$

The form of the scaling function $f(x)$ depends on details of the aggregation mechanism, which for real systems is almost unknown. A way of avoiding this problem is to choose a simple functional form for $f(x)$ that has the required limiting behaviour for $x > 1$ and $x \ll 1$ and hope that this is sufficient to fit the data. We assume for $f(x)$ a behaviour of the type

$$f(x) = f_0 \exp(-x^\beta) \qquad (15)$$

which is known as a stretched exponential, with the stretch exponent β characterizing indirectly the cluster size probability distribution $N_t(M)$. The curve-fitting approach to the data with $t = 1$ day, $c(\mathrm{HDBS}) = 6 \times 10^{-4}$ mol dm^{-3}, and $c(Mg(NO_3)_2) = 6 \times 10^{-2}$ mol dm^{-3} (figure 6), gives the data using values for the parameters f_0, ξ, β and D: $f_0 = 3{\cdot}76 \times 10^{-5}$, $\xi(t = 1 \text{ day}) = 490$ nm, $\beta = 1{\cdot}63$, $D = 2{\cdot}17$. The fractal dimension found, $D = 2{\cdot}17$, is what is expected for the lamellar phase [1], and is in full agreement with the experimentally determined value $D = 2{\cdot}16$.

The calculated values of the $p(r)$ functions are

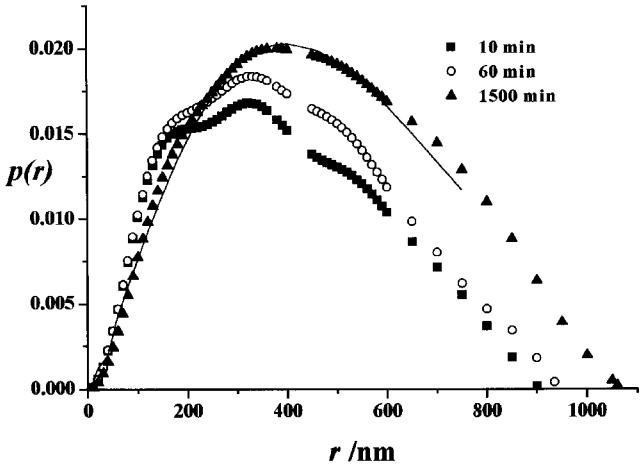

Figure 6. Pair distance distribution function for the lamellar phase of the same sample as in figure 4; in fitting curve after 1 day is shown as the unbroken line, the experimental points show the direct structure determination.

presented by the separate points in figure 6; the fitting curve uses $t = 1$ day and the size range of 10–800 nm.

Since the direct structure determination can be carried out from the pair distance distribution function [30, 31], in the system under investigation it can be recognized from the $p(r)/r = f(r)$ plot in figure 7. The thickness of a flat lamellar particle can be easily determined from the transition point, when the linearly increasing part of the curve ends. This transition occurs when the thickness of a flat particle, i.e. the thickness of the lamellae d, is equal to the radius r. From the light scattering measurements after 10 minutes and 1 day, plotting $p(r)/r = f(r)$, it can be calculated that 33 and 41 unilamellar layers stick together to form flat multi-lamellar aggregates amounting to 109 and 136 nm in thickness, respectively. The measurements after 10 and 60 minutes showed the same values for the multi-lamellar stack; the value

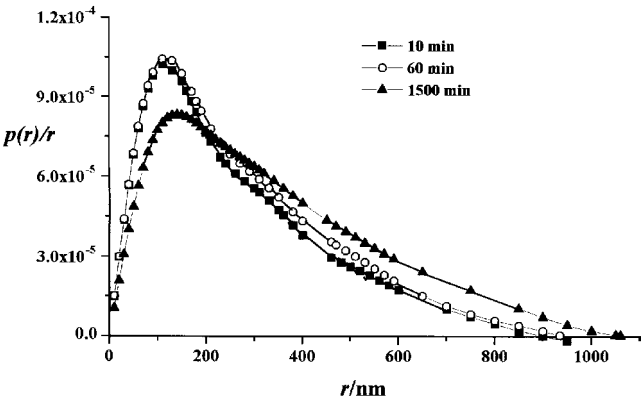

Figure 7. Pair distance distribution function divided by the particle radius enables the direct determination of the multi-lamellar thickness on the x-axes.

increased afterwards, due to the equilibration of the lamellar phase after 1 day.

4. Conclusion

In this paper the HDBS/$Mg(NO_3)_2$/water system was taken as a model for an explanation of the aggregation process following the formation of lamellar phases of ABS-compounds. Following the experimental investigation of the kinetics and structure, as well as the theoretical treatment using IFT of the light-scattering data, it was found that the self-assembly of particles in dynamic stages can be treated as a fractal object; consequently, the dynamics of formation can be mainly considered through the processes of: (i) association of molecules to form dimers and bilayers, (ii) growth of flat uni-lamellar into multi-lamellar stacks, (iii) folding of the multi-lamellar stacks into globular particles (focal-conic units), that can be considered as primary particles, (iv) aggregation of primary particles into secondary structures.

It has to be emphasized that the self-assembling nature of the amphiphile aggregation was proven by the experimental facts: the thickness of the basic uni-lamellar unit is 33 Å, the flat lamellae contain 3–4 bilayers, the multi-lamellar aggregates have 33–41 uni-lamellar units, and also the aggregation of primary or secondary particles (as observed either at the micro- or macro-level) gives the same images; in addition, the theoretical and experimental value of the effective fractal dimension for this lamellar phase was found to agree very well, $D = 2{\cdot}16$ and $D = 2{\cdot}17$, respectively. Such a fractal approach to the formation of heterogeneous systems of lamellar liquid crystals having polydisperse particles in solution has been applied here for the first time to give satisfactory agreement between experimental results and the theoretical model.

Special thanks are given to Professor A. Führer for his interest and useful discussions, and for making it possible for us to obtain the freeze etched samples and the transmission electron photomicrographs at the University of Braunschweig. Also we are obliged to Miss K. Klockers for the technical work on the FFTEM micrographs. We also express our gratitude to Dr. Stanko Popović, who obtained the X-ray diffraction patterns. The investigation was supported financially by the Ministry of Science and Technology of the Republic of Croatia.

References

[1] Težak, Đ., Martinis, M., Punčec, S., Fischer-Palković, I., and Strajnar, F., 1995, *Liq. Cryst.*, **19,** 159.
[2] Luzzatti, V., and Tardieu, A., 1974, *Ann. Rev. phys. Chem.*, **25,** 79.
[3] Saupe, A., 1977, *J. Colloid Interface Sci.*, **58,** 583.

[4] BENTON, W. J., and MILLER, C. A., 1983, *Progr. Colloid & Polym. Sci.*, **68,** 71.
[5] LARSSON, K., 1989, *J. phys. Chem.*, **93,** 7304.
[6] FONTELL, K., 1990, *Colloid Polym. Sci.*, **268,** 264.
[7] HOFFMANN, H., MUNKERT, U., THUNIG, C., and VALIENTE, M., 1994, *J. Colloid Interface Sci.*, **163,** 217.
[8] HOFFMANN, H., THUNIG, C., SCHMIEDEL, P., and MUNKERT, U., 1994, *Langmuir*, **10,** 3972.
[9] LUK, A. S., KALER, E. W., and LEE, S. P., 1993, *Biochemistry*, **32,** 6965.
[10] HOFFMANN, H., THUNIG, C., MUNKERT, U., MEYER, H. W., and RICHTER, W., 1992, *Langmuir*, **8,** 2629.
[11] DAWSON, K. A., 1992, *Pure & appl. Chem.*, **64,** 1589.
[12] SCRIVEN, L. E., 1976, *Nature*, **263,** 123.
[13] FOURNIER, J. B., and DURAND, G., 1991, *J. Phys. II France*, **1,** 845.
[14] BRAGG, W., 1934, *Nature*, **133,** 445.
[15] TEŽAK. Đ., HERTEL, G., and HOFFMANN, H., 1991, *Liq. Cryst.*, **10,** 15.
[16] TEŽAK, Đ., STRAJNAR, F., ŠARČEVIĆ, D., MILAT, O., and STUBIČAR, M., 1984, *Croat. Chem. Acta*, **57,** 93.
[17] TEŽAK, Đ., STRAJNAR, F., MILAT, O., and STUBIČAR, M., 1984, *Progr. Colloid Polym. Sci.*, **69,** 100.
[18] TEŽAK, Đ., POPOVIĆ, S., HEIMER, S., and STRAJNAR, F., 1989, *Progr. Colloid Polym. Sci.*, **79,** 293.
[19] TEŽAK, Đ., FISCHER-PALKOVIĆ, I., HEIMER, S., and STRAJNAR, F., 1992, *The Structure and Conformation of Amphiphilic Membranes*, edited by R. Lipovsky, R. Richter, and K. Kremer (Springer Verlag), p. 202.
[20] TEŽAK, Đ., 1992, *Croat. Chem. Acta*, **65,** 345.
[21] TEŽAK, Đ., and POPOVIĆ, S., 1989, *Croat. Chem. Acta*, **62,** 861.
[22] Težak, Đ., *et al.*, 1994, *Colloids Surfaces A: Physicochem. Eng. Aspects*, **90,** 261.
[23] GLATTER, O., 1977, *J. appl. Cryst.*, **10,** 415.
[24] GLATTER, O., 1980, *J. appl. Cryst.*, **13,** 577.
[25] GLATTER, O., 1982, *Small Angle X-Ray Scattering*, edited by O. Glatter and O. Kratky (London: Academic press), Chap. 4.
[26] MARTIN, J. E., and HURD, A. J., 1987, *J. appl. Cryst.*, **20,** 61.
[27] MALLAMACE, F., and MICALI, N., 1992, *Riv. Nuovo Cimento*, **15,** 1.
[28] ROBINSON, D. J., and EARNSHAW, J. C., 1993, *Phys. Rev. Letters*, **71,** 715.
[29] JU, R. T. C., FRANK, C. W., and GAST, A. P., 1992, *Langmuir*, **8,** 2165.
[30] GLATTER, O., 1990, *Neutron, X-Ray and Light Scattering: Introduction to an Investigative Tool for Colloidal and Polymeric Systems*, edited by P Lindner and Th. Zemb (New York: North-Holland), p. 49.
[31] GLATTER, O., 1991, *Progr. Collolid Polym. Sci.*, **84,** 46.